1-1-2003

Lens connexins α3Cx46 and α8Cx50 interact with zonula occludens protein-1 (ZO-1)

Peter A. Nielsen
The Scripps Research Institute

Amos Baruch
The Scripps Research Institute

Valery I. Shestopalov
Washington University School of Medicine in St. Louis

Ben N.G. Giepmans
Netherlands Cancer Institute

Irene Dunia
CNRS-Universités Paris

See next page for additional authors

Molecular Biology of the Cell
Vol. 14, 2470–2481, June 2003

Lens Connexins α3Cx46 and α8Cx50 Interact with Zonula Occludens Protein-1 (ZO-1)

Peter A. Nielsen*, Amos Baruch*¶, Valery I. Shestopalov†#, Ben N.G. Giepmans‡, Irene Dunia§, E. Lucio Benedetti§, and Nalin M. Kumar‖**

*Department of Cell Biology, The Scripps Research Institute, La Jolla, California 92037, USA., †Department of Ophthalmology and Visual Sciences, Washington University School of Medicine, St. Louis, Missouri 63110, USA., ‡Division of Cellular Biochemistry, The Netherlands Cancer Institute, Amsterdam, The Netherlands., §Institut Jacques Monod, CNRS-Universités Paris 6-Paris 7, Paris, France., ‖Department of Ophthalmology and Visual Sciences, University of Illinois at Chicago, Chicago, Illinois 60612, USA.

Submitted October 8, 2002; Revised January 20, 2003; Accepted February 26, 2003
Monitoring Editor: Daniel Goodenough

Connexin α1Cx43 has previously been shown to bind to the PDZ domain–containing protein ZO-1. The similarity of the carboxyl termini of this connexin and the lens fiber connexins α3Cx46 and α8Cx50 suggested that these connexins may also interact with ZO-1. ZO-1 was shown to be highly expressed in mouse lenses. Colocalization of ZO-1 with α3Cx46 and α8Cx50 connexins in fiber cells was demonstrated by immunofluorescence and by fracture-labeling electron microscopy but showed regional variations throughout the lens. ZO-1 was found to coimmunoprecipitate with α3Cx46 and α8Cx50, and pull-down experiments showed that the second PDZ domain of ZO-1 was involved in this interaction. Transiently expressed α3Cx46 and α8Cx50 connexins lacking the COOH-terminal residues did not bind to the second PDZ domain but still formed structures resembling gap junctions by immunofluorescence. These results indicate that ZO-1 interacts with lens fiber connexins α3Cx46 and α8Cx50 in a manner similar to that previously described for α1Cx43. The spatial variation in the interaction of ZO-1 with lens gap junctions is intriguing and is suggestive of multiple dynamic roles for this association.

INTRODUCTION

Gap junctions form channels between neighboring cells, which allow the diffusion of low-molecular-weight substances that can coordinate physiological events in tissues (Kumar and Gilula, 1996). A gap junction channel consists of two interacting hemichannels (connexons), which contain six connexin subunits each. Each connexin is a polypeptide that traverses the cell membrane four times, with both the NH_2- and COOH-termini located in the cytoplasm (Milks *et al.*, 1988; Yeager and Gilula, 1992). Connexons may consist of only one connexin isoform (homomeric) or of multiple isoforms (heteromeric). In the ocular lens, cells in the interior are dependent on gap junctional communication to maintain the ionic and water balance of the intercellular milieu, and the transparency and optical properties of the lens (Mathias *et al.*, 1997). The anterior epithelial monolayer of the lens contains gap junctions composed primarily of α1Cx43 connexin, whereas α3Cx46 and α8Cx50 connexins are coexpressed during the process of terminal differentiation and elongation of the epithelium into fiber cells. The importance of a functional gap junction network in the lens is demonstrated by targeted deletion of α3Cx46 connexin, which results in nuclear cataracts and Ca^{2+}-activated proteolysis (Gong *et al.*, 1997; Baruch *et al.*, 2001), whereas α8Cx50-knockout mice show microphthalmia and develop a pulverulent type of cataract (White *et al.*, 1998).

In lens fiber cells, α3Cx46 and α8Cx50 connexins are found in the same junctional plaque (Paul *et al.*, 1991; Dunia *et al.*, 1998) and have been reported to form heteromeric connexons (Jiang and Goodenough, 1996). In the lens cortex, these connexins are localized primarily to the broad sides of fiber cells (Gruijters *et al.*, 1987; Tenbroek *et al.*, 1992), whereas in the nuclear region, the COOH-termini of α3Cx46 and α8Cx50 connexins are proteolytically cleaved, and the

Article published online ahead of print. Mol. Biol. Cell 10.1091/mbc.E02–10–0637. Article and publication date are at www.molbiolcell.org/cgi/doi/10.1091/mbc.E02–10–0637.

Present addresses: ¶Celera Genomics, South San Francisco, CA 94080; #Bascom Palmer Eye Institute, University of Miami School of Medicine, Miami, FL 33136.

**Corresponding author. E-mail address: nalin@uic.edu.

packing arrangement of the junctional plaques is modified. This ordered distribution of gap junctions is thought to be important for maintaining lens homeostasis because of involvement in a proposed internal microcirculatory system (Mathias *et al.*, 1997). The details of how the organization and processing of lens gap junctions are achieved are unclear.

In a multitude of cellular systems containing specialized membrane domains, certain membrane channels and receptors have been demonstrated to interact with proteins containing PDZ (PSD-95, discs large, ZO-1) domains (e.g., Shaker voltage-gated K^+ channels [Kim *et al.*, 1995] and β_2-adrenergic receptors [Hall *et al.*, 1998a]). In some cases, these interactions are needed to direct the membrane proteins to the appropriate membrane subdomain (Muth *et al.*, 1998; Moyer *et al.*, 2000). Other roles for PDZ domain–containing proteins include coupling channels and transmembrane proteins to downstream signaling and cytoskeletal elements and their involvement in insertion, endocytosis, and recycling of proteins (Fanning *et al.*, 1999). Zona occludens protein-1 (ZO-1) is a member of the MAGUK (membrane-associated guanylate kinase) family and contains three PDZ domains, an Src-homology-3 (SH3) domain, and an inactive guanylate kinase (GUK) domain. The interaction of ZO-1 with the tight junction components occludin and claudins and with cadherins has been demonstrated previously (Itoh *et al.*, 1993). ZO-1 also interacts with α1Cx43 connexin (Toyofuku *et al.*, 1998) via binding of the second PDZ domain to the most COOH-terminal residues of α1Cx43 (Giepmans and Moolenaar, 1998; Giepmans *et al.*, 2001). Recently, α7Cx45 was also shown to interact with ZO-1, although it is not clear what domains are involved in this interaction (Kausalya *et al.*, 2001; Laing *et al.*, 2001).

Because of the sequence similarity between the COOH-termini of α1Cx43, α3Cx46, and α8Cx50, the expression of ZO-1 and its interaction with α3Cx46 and α8Cx50 connexins was examined in the lens.

MATERIALS AND METHODS

Northern Blot Analysis

RNA was extracted from 2- to 3-wk-old wild-type C57BL/6 mice by use of Trizol reagent (Life Technologies, Gaithersburg, MD), separated by denaturing formaldehyde gel electrophoresis, and blotted to Hybond-XL (Amersham Pharmacia, Piscataway, NJ). A probe encompassing nucleotides 0–560 of the mouse ZO-1 coding sequence was generated by RT-PCR, cloned, and sequenced. This probe was random prime–labeled using ^{32}P and hybridized to the blot at 68°C using ExpressHyb buffer (Clontech, Palo Alto, CA) according to the instructions from the manufacturer. The blot was washed to a stringency of 0.1 × SSC, 60°C, and exposed to BioMax MS film (Eastman Kodak, Rochester, NY) for 48 h at −80°C.

Antibodies

A rabbit pAb was raised against a synthetic peptide from the cytoplasmic loop of mouse α8Cx50 as described previously (White *et al.*, 1992) and affinity-purified. A rabbit pAb was raised against a synthetic peptide from the cytoplasmic loop of mouse α3Cx46 (RRDNPQHGRGREPMC) and affinity-purified. This antibody has been used in previous studies (Gong *et al.*, 1997; Dunia *et al.*, 1998). An anti–ZO-1 pAb was obtained commercially (Zymed Laboratories, South San Francisco, CA). A rat anti–ZO-1 monoclonal antibody (mAb), R26.4C (Stevenson *et al.*, 1986; Anderson *et al.*, 1988), was obtained from the Developmental Studies Hybridoma Bank developed under the auspices of the National Institute of Child Health and Human Development and maintained by The University of Iowa, Department of Biological Sciences, Iowa City, IA.

Immunoblot Analyses

Lens material was homogenized in IP buffer (50 mM Tris, 150 mM NaCl, 2 mM EDTA, 1% NP-40, 0.25% deoxycholate, pH 8.0), sonicated, and clarified by centrifugation. Samples were separated on 7% or 10% SDS-PAGE gels on a Hoefer vertical gel apparatus, followed by transfer to Protran 0.2-μm pore size nitrocellulose membranes (Schleicher & Schuell, Keene, NH). Membranes were stained with 0.2% Ponceau S in 1% acetic acid, blocked with 5% skimmed milk powder in TBST, and incubated with primary antibodies. These were detected by chemiluminescence (SuperSignal West Pico, Pierce, Rockford, IL) using goat anti-rabbit horseradish peroxidase–conjugated secondary antibodies (Bio-Rad Laboratories, Hercules, CA), followed by exposure to Biomax ML film (Eastman Kodak).

Immunostaining and Confocal Laser Scanning Microscopy

Lenses from C57BL/6 mice were fixed in 4% paraformaldahyde for 40 min, sectioned to a thickness of 150 μm with a Vibratome (model 3000, TPI, St. Louis, MO), and refixed in 4% paraformaldahyde for 30 min. For most of the colocalization stainings, rabbit pAbs were used to detect α8Cx50 and α3Cx46, as well as ZO-1, by use of a procedure that discriminated between the various antibodies. Briefly, sections were blocked with 5% goat serum in PBS, followed by application of the connexin antibody. The bound antibody was detected with goat anti-rabbit Fab fragments conjugated with rhodamine (Jackson ImmunoResearch Laboratories, West Grove, PA). Bound pAbs were then blocked with unconjugated goat anti-rabbit Fab fragments, after application of anti-ZO-1 pAbs. The bound ZO-1 antibody was then detected with Alexa 488-conjugated goat anti-rabbit IgG (Molecular Probes, Eugene, OR). Controls included incubation with either of the primary antibodies alone, followed by incubation with Alexa 488-conjugated secondary antibody, blocking with Fab fragments, and incubation with rhodamine-conjugated secondary antibody. In all cases, very little staining was observed from the rhodamine-conjugated secondary antibody, indicating that the blocking was efficient and that the labeling of individual primary antibodies was specific. Furthermore, these results were verified by substituting the rabbit pAb against ZO-1 with rat mAb R24.6C and detecting the primary antibodies with species-specific secondary antibodies. In this case, R24.6C was detected by use of goat anti-rat FITC (Southern Biotechnology Associates, Birmingham, AL). Stained preparations were imaged with a confocal microscope (LSM410, Carl Zeiss, Thornwood, NY) equipped with an argon/krypton laser.

Cell Lines. Cells were grown on poly-L-lysine–treated glass coverslips, washed in PBS, and fixed in −20°C methanol for 6 min. Coverslips were blocked with 5% goat serum in PBS (blocking buffer), followed by incubations with primary antibodies overnight in blocking buffer at 4°C. pAbs were used at 1–5 μg/ml. After washing with PBS, coverslips were incubated with fluorochrome-labeled secondary antibodies (Southern Biotech Associates, Birmingham, AL), diluted 1:100, together with 50 nM To-Pro3 (Molecular Probes, Eugene, OR), in blocking buffer. Washed slides were mounted with Fluoromount-G (Sigma, St. Louis, MO), and images were collected with a Zeiss Axiovert confocal microscope.

Electron Microscopy Freeze-Fracture Immunolabeling

Lenses for freeze-fracture immunolabeling were dissected immediately after the animals were killed. The cortical lens region was separated, and small pieces were placed on flat gold specimen holders (Balzers, Liechtenstein), frozen by quick immersion in liquid propane (Balzers), and finally stored in liquid nitrogen until replicated. Freeze-fracture was performed at −140°C in a freeze-fracture apparatus (model 301 or 400; Balzers). After fracture, the specimens were shadowed by platinum/carbon evaporation from an electron gun. The replicas were detached from the tissue by immersion in PBS, treated with 2% SDS, and processed for immunolabeling according to a technique described elsewhere (Dunia *et al.*, 2001). Replicas were examined with a Philips CM12 or Tecnai 12 electron microscope operating at 80 kV.

Immunoprecipitation

Lenses from adult wild-type C57BL/6, α8Cx50−/−, and α3Cx46−/− mice were homogenized in IP buffer, as described above. This buffer has been optimized to maximize the binding of α1Cx43 to ZO-1 while minimizing nonspecific interactions (Giepmans and Moolenaar, 1998). The clarified homogenates were incubated with either mAb R26.4C (anti–ZO-1) or normal rat serum bound to protein-G agarose. The agarose beads were washed extensively in IP buffer and eluted with SDS-PAGE sample buffer, and precipitated proteins were analyzed by immunoblotting.

Constructs

The generation of ZO-1 PDZ–GST fusion protein constructs was described previously (Nielsen *et al.*, 2002).

Oligonucleotide primers A3FOR (5′-ATGGGATCCGCAATGGGCGACTGGAGCTTCC-3′) and A3REV (5′-ATGGAATTCCTAGATGGCCAAGTCACCTGGTCTGGC-3′) were used to amplify the coding region of α3Cx46 from mouse genomic DNA by PCR. Similarly, the coding region of α3Cx46 lacking the most COOH-terminal isoleucine residue (ΔI) was amplified with primers A3FOR and A3dIREV (5′-ATGGAATTCCTAGGCCAAGTCACCTGGTCTGGC-3′). The coding region of α8Cx50 was amplified with primers A8FOR (5′-ATGGGATCCGCAATGGGCGACTGGAGTTTCC-3′) and A8REV (5′-ATGGAATTCTCATATGGTGAGATCATCTGACCTGGC-3′), and the α8Cx50ΔI construct was generated with primers A8FOR and A8dIREV (5′-ATGGAATTCTCAGGTGAGATCATCTGACCTGGC-3′). The PCR products were digested with *Bam*HI and *Eco*RI and cloned into pcDNA3 (Invitrogen, San Diego, CA). This expression vector contains a CMV promotor and a SV40 polyadenylation signal. After sequence verification, the constructs were transiently expressed in HEK293 cells.

Pull-down Experiments

Lenses from 2- to 4-wk-old wild-type C57BL/6 and α3Cx46 and α8Cx50 knockout mice were homogenized in IP buffer and clarified. GST fusion proteins containing the PDZ domains of ZO-1 were induced by standard procedures and bound to glutathione-agarose. After washing, agarose beads were incubated with equal amounts of lens homogenate. Agarose beads were then washed extensively, and fusion proteins, together with specifically bound proteins, were released from the beads with SDS-PAGE sample buffer. The samples were analyzed by immunoblotting. Membranes were stained with Ponceau S to verify that equal amounts of the PDZ1-, 2-, and 3-GST fusion proteins had been incubated with lens homogenates.

RESULTS

ZO-1 Expression in the Lens

Because ZO-1 expression has not previously been examined in the lens, the ZO-1 RNA levels in lens and other tissues from adult C57BL/6 mice were examined by Northern blot analysis. The lens ZO-1 RNA expression levels (Figure 1A, lane 1) were found to exceed the ZO-1 RNA levels from testis, heart, brain, and kidney (Figure 1A, lanes 2–5), tissues known to express ZO-1 protein. The transcript size of ZO-1 RNA was slightly larger in the lens than in the other organs examined. This most likely represents alternative splicing of the transcript, because multiple splice variants of ZO-1 are found in various tissues (Gonzalez-Mariscal *et al.*, 1999).

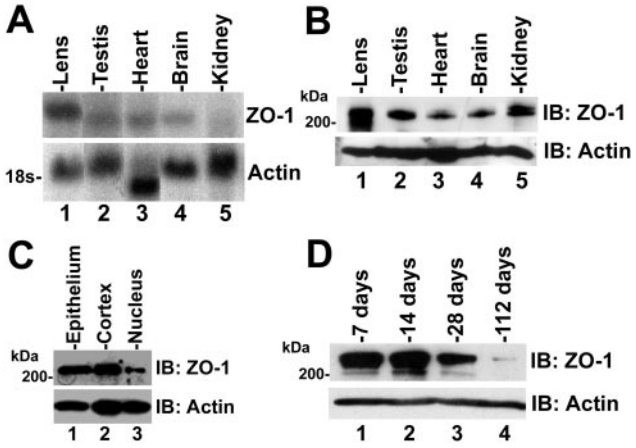

Figure 1. ZO-1 is expressed in all regions the mouse lens in an age-dependent manner. (A) Northern blot analysis of lens, testis, heart, brain, and kidney from adult wild-type (wt) C57 mice probed for ZO-1 (top) and actin (bottom). ZO-1 RNA was highly expressed in the whole lens. (B) Immunoblot analysis of ZO-1 expression from mouse lens, testis, heart, brain, and kidney (top) and actin (bottom). ZO-1 was found to be expressed significantly in the lens compared with the other tissues. (C) Immunoblot analysis of ZO-1 expression in different regions of adult mouse lenses. The lens epithelial (lane 1), cortical (lane 2), and nuclear (lane 3) layers were separated by microdissection. ZO-1 was detected in all regions of the lens (top). The blot was reprobed for actin expression (bottom). (D) Immunoblot analysis of lens ZO-1 levels at different ages. ZO-1 levels decreased several-fold in adult lenses (top). Reprobing of the blot for actin showed that equal amounts of proteins were analyzed (bottom). The faster-migrating form of actin observed in heart probably corresponds to a splice variant that has been described previously (Pari *et al.*, 1991).

ZO-1 protein levels were then analyzed by immunoblot of lysates from several mouse tissues (Figure 1B) and were found to correlate well with the respective ZO-1 RNA levels in Figure 1A, confirming that significant amounts of ZO-1 were expressed in lens (Figure 1B).

In these studies, whole lenses were analyzed. These contain at least three regions, epithelium, cortical fibers, and nuclear fibers, with cells at different stages of differentiation. To determine the proportion of ZO-1 in each of these regions, mouse lenses were microdissected to enrich for the respective layers, and the fractions were analyzed by immunoblot. ZO-1 was found in all regions of the mouse lens, although more abundantly in the epithelial and differentiating, cortical fiber cell layers (Figure 1C, lanes 1–2) than in the mature, nuclear fiber cells (Figure 1B, lane 3). Furthermore, immunoblot analysis of whole lenses from 1-, 2-, 3-, and 16-wk-old mice revealed that ZO-1 levels decreased drastically 3 wks after birth (Figure 1D).

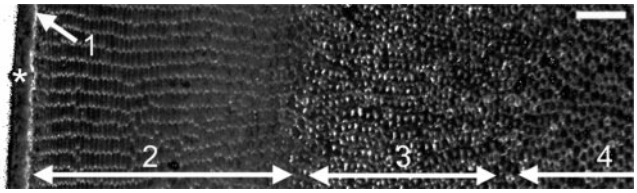

Figure 2. Expression pattern of ZO-1 in mouse lenses. The epithelium at the surface of the lens is indicated by an asterisk. The ZO-1 localization changes throughout zones of the lens (indicated by numbers). Intense ZO-1 staining is seen at the epithelium–fiber cell interface (1). In the outer cortex (2), ZO-1 is located primarily at the narrow face of fiber cells. In midcortex (3), ZO-1 is localized primarily to the broad face at fiber cells. In deep cortex (4), ZO-1 is more uniformly distributed on the membrane. Bar, 25 μm.

Localization of ZO-1 and Connexins in the Lens

Mouse lenses were sectioned in the equatorial plane and examined by immunofluorescence-scanning confocal microscopy with two different antibodies against ZO-1. These two antibodies gave similar staining patterns. Distinct zones with different ZO-1 staining patterns were discernible in the lens and are labeled by numbers (1–4) in Figure 2. A description of the observed results in the different zones is given below.

Zone 1. At the epithelium–fiber interface, an intense punctate staining at the apical side of the epithelial cells was observed from the proliferative region to the equator. At high magnification, a punctate staining was also observed at cell–cell contacts between epithelial cells. Similar staining was also observed at cell–cell contacts between the posterior tips of elongating fibers. It is noteworthy that such punctuate staining of ZO-1 at the fiber cell tips was observed only at the posterior part of the lens. At the corresponding domain of the epithelial cell membrane, staining for ZO-1 was not observed (our unpublished results).

Zone 2. In outer cortical fibers cells, 10–150 μm from the surface, a punctate membrane staining with spots predominantly at the narrow faces of fiber cell hexagons was observed. For a few outer cell layers, small, scattered punctuate spots of ZO-1 were seen at the broad face of fiber cells, but these disappeared by 30–40 μm and deeper (our unpublished results).

Zone 3. At 175–300 μm from the surface (midcortex), ZO-1 appeared to translocate from the narrow side of fiber cells, to localize predominantly to the broad face of fiber cells.

Zone 4. At 325–425 μm from the surface (deep cortex), ZO-1 appeared to be more evenly distributed on both narrow and broad sides of fiber cells, although these are more irregular at this location.

In the nuclear region, a diffuse staining of the plasma membrane was observed. At high magnification, however, it became apparent that ZO-1 staining was not uniform across the fiber cell membrane, showing limited areas of decreased staining. Because of the extensive proteolysis and exposure of cryptic epitopes in the nucleus, it is not clear whether the staining observed in the nucleus represents intact ZO-1, fragments of ZO-1, or cross-reactivity of the antibodies (our unpublished results).

The colocalization of ZO-1 with α3Cx46 and α8Cx50 connexins in mouse lens sections was then examined (Figure 3). In the outer cortex (corresponding to zone 2 in Figure 2, 10–150 μm from the surface), ZO-1 and α3Cx46 connexins are located primarily on different faces of hexagonal fiber cells: ZO-1 was observed on the narrow faces, whereas α3Cx46 connexins localized to the broad faces of fiber cells (Figure 3, A–C; detail in Figure 3, D–F). In the midcortex (corresponding to Zone 3 in Figure 2, 175–300 μm from the surface) and continuing into the deep cortex (corresponding to Zone 4 in Figure 2, 325–425 μm from the surface), ZO-1 was observed to colocalize extensively with α3Cx46 on the broad faces of fiber cells (Figure 3, G–I). Furthermore, at the lens periphery, some colocalization at the fiber–epithelium interface and the lateral membrane was observed (our unpublished results).

Similarly to α3Cx46, α8Cx50 connexin was observed to colocalize extensively with ZO-1 in both mid and deep cortex but rarely in the outer cortex, where α8Cx50 was also located primarily at the broad faces of fiber cell hexagons (Figure 3, J–L).

Topographic distribution of ZO-1 and α3Cx46 and α8Cx50 Connexins as Revealed by Fracture-Labeling

Electron microscopy analysis of fracture-labeling (FL) of lenses performed with either anti-α3Cx46 or anti-α8Cx50 connexin antibodies, or both, indicated that these connexins are the major constituents of the nascent junctional domains (linear strands or small packed arrays of 9-nm junctional intramembranous particles). On the protoplasmic fracture face (PF), the fracture exposed large aggregates of 9-nm intramembranous particles and the corresponding pits on the exoplasmic fracture face (EF), which are a characteristic of gap junctions. The fiber connexins appeared codistributed on the same junctional plaque. Double-gold immunolabeling with anti-α3Cx46 or anti-α8Cx50 and anti-ZO-1 antibodies demonstrated that both ZO-1 and connexins could be detected in the same junctional plaque (Figure 4A). At more advanced stages of junctional assembly, double-gold immunolabeling with anti–ZO-1 antibodies and anti-α3Cx46 (Figure 4B) or anti-α8Cx50 (Figure 4C) indicated that ZO-1 is randomly distributed within the junctional plaque. In a few junctional domains, the gold-labeled ZO-1 appeared preferentially packed at the periphery of the junctional plaque. However, ZO-1 does not form a crown of labeled particles along the edge between EF and PF as has been described previously for MP26 (Dunia *et al.*, 1998).

FL on Lens Fiber Cells from Mice Lacking Either α3Cx46 or α8Cx50 Connexins

Targeted gene ablation of lens connexin produces two different phenotypes: a nuclear cataract in α3Cx46 ($-/-$) mice and a microphthalmia associated with a pulverulent type of cataract in α8Cx50 ($-/-$) mice. The topographic distribution of the immunogold-labeled ZO-1 in the lens fiber cells of each of the connexin knockout mice is comparable to that described above for wild-type mouse lenses. Thus, double-immunogold labeling using anti-α3Cx46 or anti-α8Cx50 and anti-ZO-1 antibodies, respectively, indicated that ZO-1 remains in close topographic association with the junctional plaques irrespective of whether they contained homomeric–homotypic α8Cx50 connexons (α3Cx46$-/-$) (Figure 4D) or homomeric–homotypic α3Cx46 connexons (α8Cx50 $-/-$) (Figure 4E).

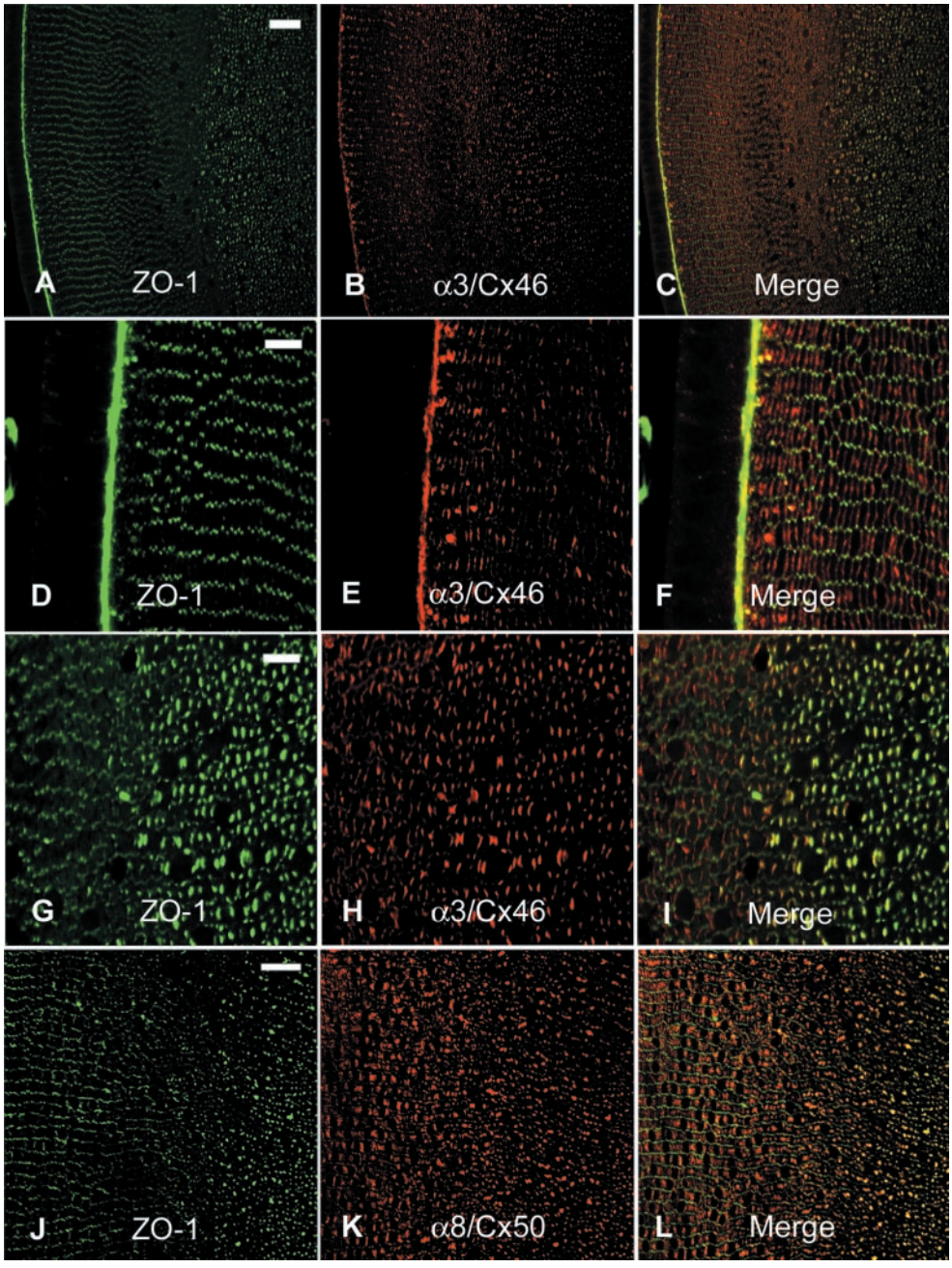

Figure 3. ZO-1 partially colocalizes with α3Cx46 and α8Cx50 in wild-type (wt) mouse lenses. Panels A–C, D–F, G–I, and J–L each represent one double-labeled section, with each row of three images showing ZO-1 staining (left column), connexin staining (middle column; α3Cx46 in B, E, and H and α8Cx50 in K), and the merged staining (right column). The lens epithelium is seen to the left in all panels. (A–C) Overview showing the outer and middle cortex. In the outer cortex, ZO-1 and α3Cx46 show very limited colocalization, whereas extensive colocalization is observed in the midcortex. Bars, 25 μm. (D--F) Detail showing the epithelium–fiber interphase and outer cortex. ZO-1 localizes primarily to the narrow faces of fiber cell hexagons, whereas α3Cx46 is localized primarily to the broad faces of fiber cells. Bars, 10 μm. (G–I) Detail showing the transition zone between outer cortex and midcortex. ZO-1 appears to translocate from the narrow face of fiber cells to the broad face and is observed to colocalize extensively with α3Cx46. Bars, 10 μm. (J–K). Overview showing the ZO-1 and α8Cx50 distribution in the lens cortex. The colocalization is limited in the outer cortex but extensive in the midcortex region. Bars, 25 μm.

Coimmunoprecipitation of ZO-1 and Lens Connexins

To determine whether ZO-1 interacts with α3Cx46 and α8Cx50 in mouse lenses, immunoprecipitated ZO-1 from mouse lenses was analyzed by immunoblotting using specific connexin antibodies. These experiments demonstrated that α3Cx46 was coprecipitated with ZO-1 from total lens lysates (Figure 5A, lane 3) but not with an irrelevant antibody (Figure 5A, lane 2). A similar coimmunoprecipitation of α3Cx46 with ZO-1 was observed with lens lysates prepared from α8Cx50 knockout mice (Figure 5A, lane 4), suggesting that this is a result of direct interactions with α3Cx46 connexin and not of heteromeric gap junctions of α3Cx46 and α8Cx50 connexins that may exist in the lens. Reprobing of the blot showed that ZO-1 was present in both immunoprecipitations, as expected (Figure 5A, bottom). A similar immunoprecipitation of ZO-1 from wild-type mouse lenses and from α3Cx46 knockout lenses showed that α8Cx50 connexin also coprecipitated with ZO-1 but not with an irrelevant antibody (Figure 5B). Ponceau staining of the blot showed that equal amounts of anti–ZO-1 and irrelevant antibody had been used for the immunoprecipitation (Figure 5B, bottom).

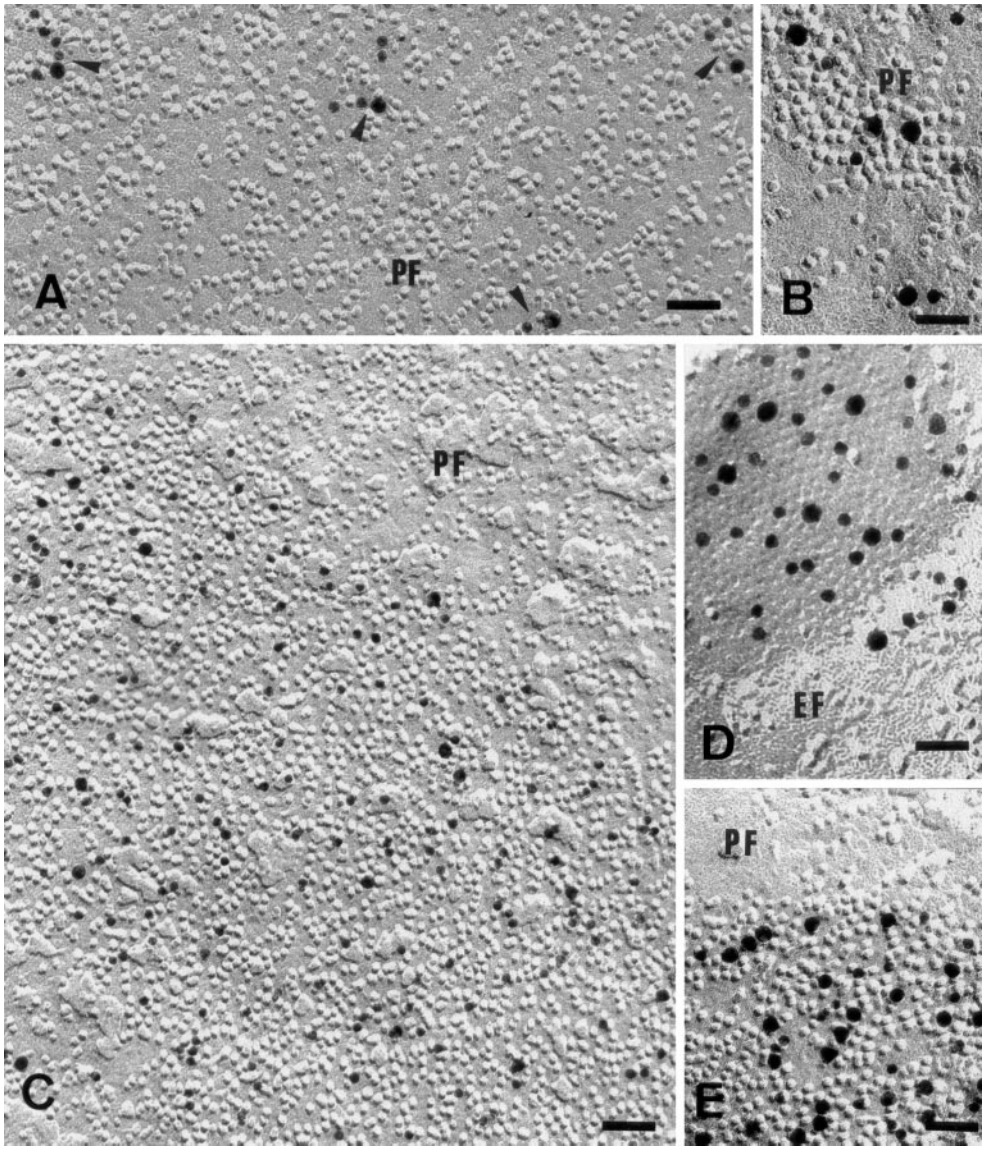

Figure 4. FL of differentiating lens fiber cell plasma membranes of wild-type (wt) and connexin knock-out mice. PF, Protoplasmic fracture face; EF, exoplasmic fracture face. (A) Wt mouse lens. Double-immunolabeling with antibodies directed against α8Cx50 (10-nm gold particles) and ZO-1 (15-nm gold particles). On PF, small clusters of junctional particles (arrowheads) are labeled with α8Cx50 antibody. Note that ZO-1 immunolabeling is distributed strictly in association with initial sites of junctional assembly. Bar, 60-nm. (B) Wt mouse lens. Double-immunolabeling with antibodies directed against α3Cx46 (10-nm gold particles) and ZO-1 (15-nm gold particles). Immunolabeled ZO-1 is associated with clusters of junctional intramembranous particles (IMP) composing α3Cx46, visualized on PF. Bar, 38 nm. (C) Wt mouse lens. Double-immunolabeling with antibodies directed against α8Cx50 (10-nm gold particles) and ZO-1 (15-nm gold particles). PF displays a large packing of junctional IMP labeled by anti-α8Cx50 antibody. Note that the immunolabeled ZO-1 is restricted to the junctional plaque and codistributed with α8Cx50. Bar, 55 nm. (D) Knock-out α3Cx46 mouse lens. Double-immunolabeling with antibodies directed against α8Cx50 (10-nm gold particles) and ZO-1 (15-nm gold particles). The fracture has exposed the EF of a large junctional plaque. Immunolabeling is restricted to the junctional domain. Bar, 38 nm. (E) Knock-out α8Cx50 mouse lens. Double-immunolabeling with antibodies directed against α3Cx46 (10-nm gold particles) and ZO-1 (15-nm gold particles). The fracture has exposed a PF displaying loosely packed junctional particles. α3Cx46 and ZO-1 are codistributed. Bar, 45 nm.

The Second PDZ Domain of ZO-1 Interacts with Lens Connexins

The different PDZ domains of ZO-1 were analyzed for their involvement in the interaction with α3Cx46 and α8Cx50 connexins. Lysates from mouse lenses were used in pull-down experiments with the three separate ZO-1 PDZ domains expressed as GST fusion proteins, and the lens connexins bound to the fusion proteins were detected by immunoblot analysis. Using the second PDZ-domain of ZO-1, a signal for both α3Cx46 (Figure 6A, lane 3) and α8Cx50 (Figure 6B, lane 3) was observed, suggesting its involvement in the interaction with lens gap junctions. No interaction between lens connexins and the first or third PDZ domain was detected (Figure 6, A and B). Ponceau staining of the blot showed that equal amounts of PDZ-GST fusion proteins were used in all pull-down experiments (Figure 6, A and B, bottom). To determine whether these results were a result of the presence of the other connexin isoform in a heteromeric connexon, similar pull-down assays were performed using the second PDZ domain and lens lysates from α3Cx46 and α8Cx50 knockout mice. As expected, α3Cx46 was detected in α8Cx50 knockout lenses (Figure 6C, lane 2) but not α3Cx46 knockout lenses (Figure 6C, lane 1). Pull-down experiments with the second PDZ domain and lens lysates from these knockouts showed that α3Cx46 could bind to the second PDZ do-

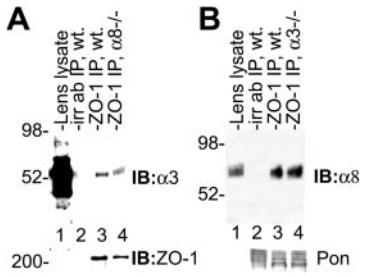

Figure 5. α3Cx46 and α8Cx50 coimmunoprecipitate with ZO-1 from mouse lens lysates. An anti–ZO-1 antibody was used for immunoprecipitation of lens lysates, and precipitates were analyzed for α3Cx46 or α8Cx50. (A) Top, immunoblot to detect α3Cx46 in wild-type (wt) mouse lenses (lane 1), immunoprecipitates of wt lenses with an irrelevant rat antibody (lane 2), immunoprecipitates of wt lenses with an anti–ZO-1 mAb (lane 3), and immunoprecipitates of α8Cx50−/− lenses with an anti–ZO-1 mAb (lane 4). α3Cx46 was coprecipitated with ZO-1 in both wt and α8Cx50−/− lenses. Bottom, immunoblot to detect ZO-1 in immunoprecipitates. Equal amounts of ZO-1 were detected in the samples containing wt and α8Cx50−/− lenses. (B) Top, immunoblot to detect α8Cx50 in wt mouse lenses (lane 1), immunoprecipitates of wt lenses with an irrelevant rat antibody (lane 2), and immunoprecipitates of wt lenses (3) and α3Cx46−/− lenses (4) with an anti–ZO-1 mAb. α8Cx50 was coprecipitated with ZO-1. Bottom, Ponceau staining of the blot to visualize antibodies. Similar amounts of irrelevant and anti–ZO-1 antibodies were used in the immunoprecipitations.

main in the absence of α8Cx50 (Figure 6C, lane 4). Similarly, α8Cx50 was found to bind to the second PDZ domain in the absence of α3Cx46 (Figure 6D, lane 3), excluding the possibility that the binding was a result of the presence of α3Cx46 in heteromeric connexons. The presence of equal amounts of PDZ2-GST fusion protein in the pull-down assays was demonstrated by Ponceau staining of the blot (Figure 6, C and D, bottom).

The COOH-Terminal Residues of Lens Connexins Bind to ZO-1

It has been demonstrated previously that the most COOH-terminal residue is involved in the interaction of α1Cx43 with ZO-1, because deleting this residue abolishes binding (Giepmans and Moolenaar, 1998). To determine the involvement of the most COOH-terminal domains of lens connexins in the interaction with ZO-1, constructs encoding mouse α3Cx46 and α8Cx50 and mutants of these lacking the most COOH-terminal isoleucine residues (α3Cx46ΔI and α8Cx50ΔI) were generated and transiently overexpressed in HEK293 cells. Immunofluorescence examination of these cells using anti-connexin antibodies revealed fluorescent spots consistent with the formation of gap junctions between two adjoining cells at sites of cell–cell contact of some cell pairs expressing either α3Cx46 (Figure 7A, arrow) or α3Cx46ΔI (Figure 7B, arrow). Similar immunofluorescent staining was detected between some cell pairs expressing either α8Cx50 or α8Cx50ΔI (Figure 7, C and D, arrows), indicating that these mutants retain the ability to traffic and assemble into what are probably gap junctions in HEK293 cells. Some cell pairs overexpressing either the wild-type or mutated connexins showed intense fluorescence spread all over the plasma membrane and accumulation within cellular compartments, most likely because of high levels of connexin protein expressed in these cells (Figure 7D).

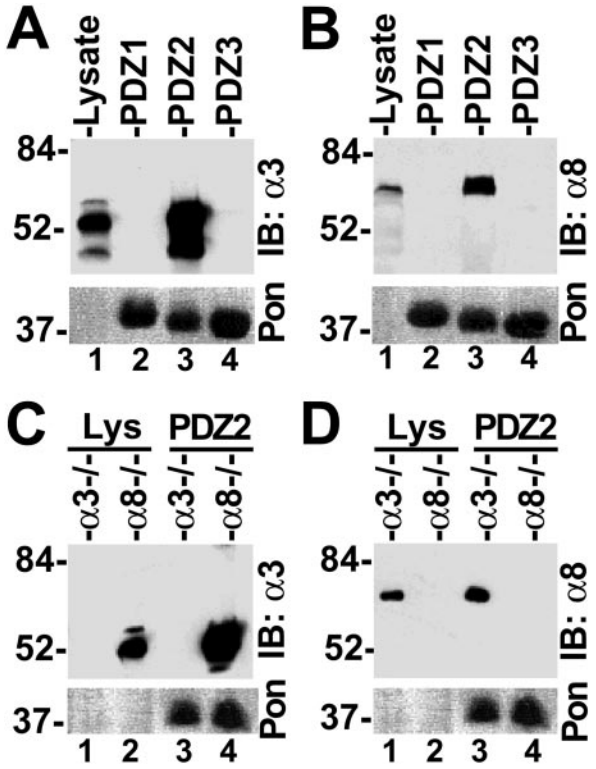

Figure 6. The second PDZ domain of ZO-1 binds α3Cx46 and α8Cx50 independently. Immunoblot analysis of pull-down experiments in which mouse lens homogenates were incubated with ZO-1 PDZ domains. PDZ domains were fused to GST and expressed in bacteria. Lens homogenates from adult wild-type (wt) C57 mice incubated with the first, second, and third PDZ domains were examined for α3Cx46 binding (A) and α8Cx50 binding (B) (tops). Binding to the second PDZ domain of ZO-1 was observed for both connexins. Ponceau staining of the membrane showed that equal amounts of each PDZ domain containing fusion protein had been used (bottom). (C and D) Lens homogenates from adult mixed background α3Cx46 and α8Cx50 knockout mice incubated with the second PDZ domain were examined for α3Cx46 binding (C) and α8Cx50 binding (D) (top). Binding of α3Cx46 in α8Cx50 knockouts (A) and of α8Cx50 in α3Cx46 knockouts (B) was observed. Ponceau staining of the membrane showed that equal amounts of PDZ2 fusion protein had been used (bottoms).

When homogenates of these cells were analyzed by immunoblotting using connexin antibodies, products were detected for all four constructs but not in wild-type HEK293 cells, as expected (Figure 8, A and B, bottom). However, analysis of homogenates from cells transfected with α3Cx46 and α3Cx46ΔI indicated the presence of several products, most of which migrated slightly faster than lens α3Cx46 in SDS-PAGE (Figure 8A, bottom, lanes 3 and 4, arrow). In contrast, a single connexin band was observed by SDS-PAGE in homogenates from cells expressing α8Cx50 and α8Cx50ΔI after short exposure. The SDS-PAGE mobility of this band was similar to the upper, major band of α8Cx50 from lens lysate (Figure 8B, bottom, lanes 3 and 4). Ponceau staining of the blots showed that equal amounts of lens,

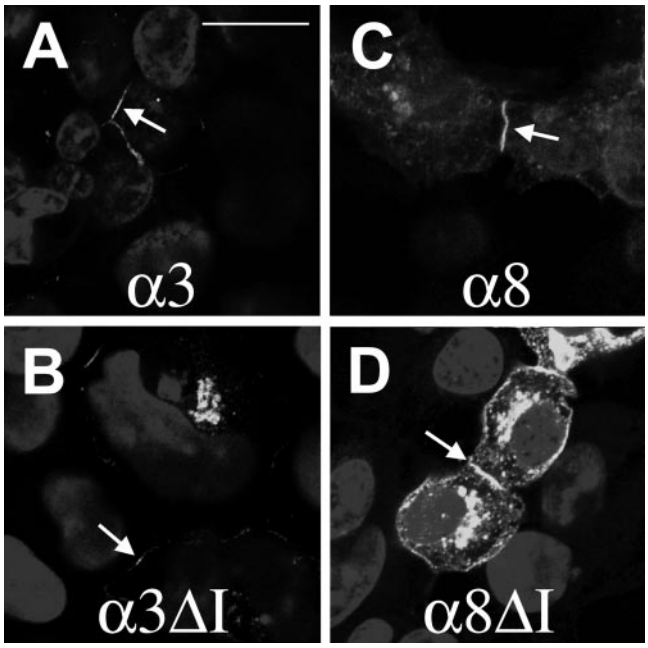

Figure 7. Wild-type (wt) α3Cx46 and α8Cx50 and mutants of these lacking the most COOH-terminal isoleucine residues (α3Cx46ΔI, α8Cx50ΔI) can form structures resembling gap junctions in cell culture. Immunoconfocal analyses of transiently overexpressed wt α3Cx46 (A), α3Cx46ΔI (B), wt α8Cx50 (C), and α8Cx50ΔI (D) in HEK293 cells. Nuclear staining is superimposed on the immunofluorescent staining. Various levels of connexin expression are seen because of the transient expression. Structures resembling gap junctions are seen between cells for both wt and mutated connexins (arrows). Bar, 20 μm; all panels are the same magnification.

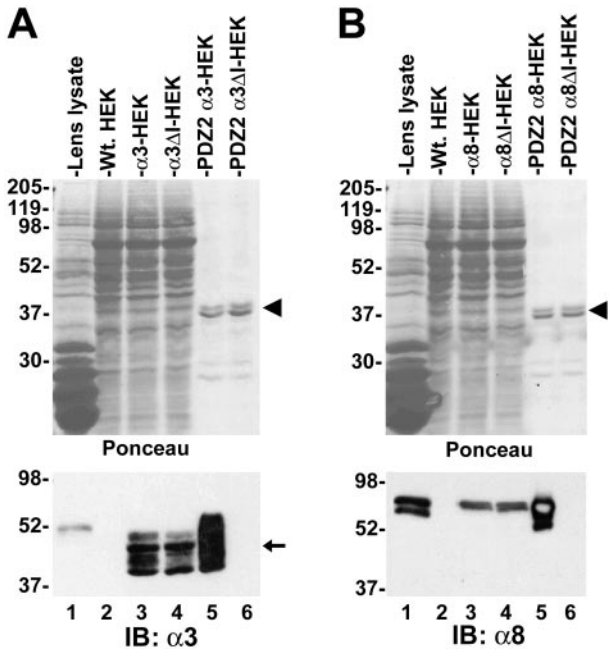

Figure 8. The most COOH-terminal isoleucine residue of connexins α3Cx46 and α8Cx50 are required for binding to the second PDZ domain of ZO-1. Lysates from HEK293 cells transiently overexpressing α3Cx46, α3Cx46ΔI, α8Cx50, and α8Cx50ΔI were incubated with the second PDZ domain of ZO-1 expressed as a bacterial GST fusion protein. (A) Immunoblot analyses of α3Cx46 and α3Cx46ΔI binding to PDZ2. Ponceau staining of the blot (top) showed that comparable amounts of mouse lens lysate (lane 1), wild-type (wt) HEK293 lysate (lane 2), lysate from HEK cells overexpressing α3Cx46 (lane 3), and lysate from HEK cells overexpressing α3ΔI (lane 4) were analyzed. Furthermore, similar amounts of PDZ2 fusion protein were used for the pull-down experiments (lanes 5 and 6, arrowhead). Immunoblotting for α3Cx46 showed that overexpressed α3Cx46 and α3Cx46ΔI migrated faster than wt α3Cx46 from lens lysate (arrow). However, overexpressed α3Cx46 bound to PDZ2, whereas α3Cx46ΔI did not. (B) Immunoblot analysis of α8Cx50 and α8Cx50ΔI binding to PDZ2. The experiment was carried out as described above, with overexpression of α8Cx50 and α8Cx50ΔI instead of α3Cx46 and α3Cx46ΔI. Overexpressed α8Cx50 and α8Cx50ΔI migrated similarly to wt α8Cx50 from mouse lens lysates. Binding of α8Cx50 but not of α8Cx50ΔI to PDZ2 was observed (bottom).

wild-type HEK293, and transfected HEK293 lysates were analyzed (Figure 8, A and B, top). Homogenates from HEK293 cells overexpressing both the wild-type and mutant connexins were then used in pull-down assays with the second PDZ domain of ZO-1 fused to GST. These experiments demonstrated that both wild-type α3Cx46 and wild-type α8Cx50, overexpressed in HEK cells, bound to the second PDZ-domain as expected (Figure 8, A and B, bottom, lanes 5). In contrast, neither α3Cx46ΔI nor α8Cx50ΔI bound to the second PDZ-domain (Figure 8, A and B, lane 6). Ponceau staining of the blot showed that equal amounts of PDZ2 had been used for the pull-down experiment (Figure 8, A and B, top, lanes 5 and 6, arrowhead).

These results indicated that the most COOH-terminal isoleucine residues in both connexins were involved in the interaction with ZO-1. Interestingly, for α3Cx46, a shorter exposure of the blot showed that primarily the slowest-migrating forms of α3Cx46 in SDS-PAGE bound to PDZ2. These connexin isoforms were thus enriched for in the pull-down assay, because they could be discerned only in the total cell lysates on longer exposure (our unpublished results). In contrast, the fastest-migrating forms, which were the most abundant forms observed in the cell lysate (Figure 8, bottom, arrow), were underrepresented in the pull-down. A possible explanation for this could be that most α3Cx46 is proteolytically cleaved in HEK293 cells, which would explain the much faster mobility compared with the lens lysate isoform. This cleavage takes place from the COOH-terminus of α3Cx46, similar to the proteolytic cleavage observed in mature layers of older lenses. In this case, the cleaved isoforms would be expected to be underrepresented or absent in the PDZ2 pull-down because of their lack of PDZ binding domain. Their presence in the pull-down, however, may be a result of their presence in connexons containing some proportion of the full-length connexin isoforms.

In contrast to α3Cx46, the amount of the faster-migrating isoform of α8Cx50 in the PDZ2 pull-down was approximately similar to the amount present in the cell lysate, as seen after longer exposure of the blot (our unpublished results). One possible explanation for this is that the two isoforms of α8Cx50 differ only in phosphorylation, which potentially does not affect binding to PDZ2.

DISCUSSION

In the present study, ZO-1 was found to be highly expressed in the lens and was found to associate with lens connexins α3Cx46 and α8Cx50 via a molecular interaction involving the second PDZ domain of ZO-1 and the most COOH-terminal residue of each connexin.

Expression and Topographic Distribution of ZO-1, α3Cx46, and α8Cx50 in the Lens

Because ZO-1 has been found primarily in association with tight junctions, which are present in the lens only at the epithelium–fiber interface, at least in some species (Zampighi *et al.*, 2000), it was surprising that lens contained high levels of ZO-1 RNA and protein compared with other organs.

In the outer cortex, ZO-1 is found primarily at the narrow faces of fiber cells, whereas in mid to deep cortex, ZO-1 is translocated to the broad face of fiber cells. In accordance with this finding, double-immunofluorescence staining revealed that ZO-1 is colocalized with lens fiber cell connexins α3Cx46 and α8Cx50 to various extents in different regions of the lens. The colocalization ranged from limited in the outer cortex to more extensive in the midcortex. The colocalization was observed primarily at junctional domains on the broad faces of fiber cells and not on the narrow faces of the fibers, which contain a limited number of gap junctions. These findings are consistent with the relatively low amount of lens connexins that coimmunoprecipitated with ZO-1 in our experiments, in which whole lenses were used. The extent of colocalization between α1Cx43 and ZO-1 in cardiac myocytes has also been reported to be limited (Barker *et al.*, 2002), suggesting that in the lens and heart, a large proportion of the connexin pool does not interact stably with ZO-1, and vice versa.

It is likely that ZO-1 interacts with other proteins besides connexins in the lens, as has been demonstrated in other cell and tissue types. Thus, ZO-1 has been reported to interact with, e.g., catenin (Rajasekaran *et al.*, 1996), JAM (Bazzoni *et al.*, 2000), cadherins (Itoh *et al.*, 1993), and actin filaments (Itoh *et al.*, 1997). Interestingly, the high levels of ZO-1 detected in lens epithelial cells by immunoblot analysis was found by immunofluorescence to localize primarily to the apical side of these cells, i.e., at the epithelium–fiber interface. It is a distinct possibility that ZO-1 in these cells interacts with α1Cx43, but ZO-1 probably also interacts with adhesion molecules that anchor the epithelial cell layer to the fiber cells. Furthermore, actin is an integral constituent of the plasma membrane–cytoskeleton complex of lens fibers. To verify and further examine the presence of ZO-1 in cortical fiber cells, fiber ghost cell preparations containing the plasma membrane cytoskeleton (Benedetti *et al.*, 1996) were stained for ZO-1. ZO-1 was found to show a patchy distribution along the fiber cell plasma membrane and forming a row of variously sized plaques in the membrane profile between two adjoining fiber cells (our unpublished results). These findings demonstrate that ZO-1 remains associated with the fiber cell ghost preparation after extraction of the water-soluble fiber constituents, suggesting that ZO-1 may be part of the plasma membrane–cytoskeleton complex. ZO-1 is probably not involved in anchoring gap junctions to the cytoskeleton in the rodent lens, because only primate and human lenses show association between gap junctions and actin filament bundles, whereas rodent lenses do not (Lo *et al.*, 1994).

Potentially, ZO-1 could coordinate the organization of specialized membrane domains and/or signaling mechanisms, because other members of the MAGUK family are implicated in the control and assembly of specialized membrane domains (Fanning *et al.*, 1998; Fanning and Anderson, 1999; Baruch and Lim, 2001). In the heart, α1Cx43 connexin is localized primarily to the intercalated disk in cardiac myocytes, and it is thought that interaction between α1Cx43 and ZO-1 is needed to localize the connexin to this specialized membrane domain (Toyofuku *et al.*, 1998). A similar localization of gap junctions to unique membrane domains is also found in, e.g., polarized thyroid epithelial cells (Guerrier *et al.*, 1995) and in the lens, in which gap junctions in the cortex localize primarily to the broad face of lens fiber cells. It is interesting that we observed only limited colocalization of ZO-1 with α3Cx46 or α8Cx50 in the outer cortex, which is the region of the lens in which gap junction plaques are organized, whereas more extensive colocalization was observed in midcortex, in which mature gap junction plaques are present. One explanation for this could be that the association of ZO-1 with α3Cx46 or α8Cx50 has diverse roles in the different regions of the lens. Perhaps only limited amounts of ZO-1 are necessary to organize and direct the gap junctional plaques to their correct membrane localization in the outer cortex, if ZO-1 is even involved in this process. In contrast, it is striking that the more extensive association between ZO-1 and α3Cx46 and α8Cx50 deeper in the cortex occurs at a stage of lens fiber development that precedes the proteolytic cleavage of the COOH-terminal of both α3Cx46 and α8Cx50. One intriguing possibility is that ZO-1 binding to lens connexins may be involved in coordinating or targeting the activities of proteolytic enzymes or kinases involved in these posttranslational modifications in this region of the lens. The molecular mechanisms involved in this process, including how ZO-1 translocates from the narrow faces of fiber cells to gap junctions, remain to be elucidated.

The results of FL experiments provided direct evidence that ZO-1 is distributed in close topographic association with α3Cx46 and α8Cx50 connexins. Furthermore, these experiments show that the interaction between ZO-1 and connexins is resistant to mild SDS treatment. Junctional constituents probably form a stable scaffold associated specifically with sites of initiation and progressive packing of the junctional domains. However, we cannot exclude the presence of an SDS-soluble pool of ZO-1 that is not revealed by FL and that could be associated with other membrane domains. This could explain the apparent discrepancy between our FL and immunofluorescence results concerning the overall localization of ZO-1, because the latter technique, using chemically fixed sections, showed additional labeling of ZO-1 at nonjunctional membrane domains of fiber cells.

During elongation and terminal differentiation of the lens fibers, several membrane and cytoskeletal proteins are expressed, in particular, the major transmembrane protein of the fibers, MP26 (MIP or Aquaporin 0), which has a dual function of water transporter and adhesion molecule (Benedetti *et al.*, 2000). FL experiments have demonstrated that MP26, during the packing of α3Cx46 and α8Cx50 con-

nexons, forms a belt of transmembrane-linked pairs around the junctional plaques. FL of ZO-1 shows that this protein does not form a crown around the junctional plaque but rather appears scattered randomly within the plaque surface. This topographic distribution is suggestive of a more general role in gap junction assembly, such as interacting with cytoskeletal constituents and/or recruiting of signaling molecules to the junctional domain.

FL experiments on lens fiber cells of α3Cx46 or α8Cx50 connexin knock-out mice showed that either connexin can be associated with ZO-1. Hence, in agreement with our biochemical data, the presence of heteromeric and/or heterotypic connexons is not required for the ZO-1–connexin interaction.

Molecular Interactions between ZO-1 and α3Cx46 and α8Cx50 Connexins

The molecular mechanism of ZO-1 interaction with α3Cx46 and α8Cx50 is apparently similar to the interaction described for α1Cx43, involving the second PDZ domain of ZO-1 and the most COOH-terminal connexin residues (Giepmans and Moolenaar, 1998; Giepmans *et al.*, 2001). The consensus motifs for PDZ-binding are the COOH-terminal sequences E-S/T-X-V/I (type I), Φ-X-Φ (type II), Φ/Ψ-X-Φ (type III) (Songyang *et al.*, 1997; Dev *et al.*, 2001), and X-D-X-V (type IV [Sheng and Sala, 2001]), where Φ is a hydrophobic residue and Ψ is a basic residue. α1Cx43 and mouse α3Cx46 and α8Cx50 connexins have a potential type II PDZ-binding domain at their COOH-termini. Furthermore, the COOH-terminal sequences of these connexins have similar but not identical residues conserved between species. For example, the COOH-terminal sequence of α3Cx46 connexin is D-L-A-I in human and rat, whereas it is D-L-A-V in Cx56, the chicken orthologue of α3Cx46. The same V-I exchange can be found in orthologues of α8Cx50, where the human sequence is D-L-T-V, whereas the mouse sequence is D-L-T-I. Because both valine and isoleucine residues in position 0 can bind type I PDZ-domains, we would not expect these sequence variations to affect binding to ZO-1.

We have recently shown that α11/Cx31.9 connexin binds to ZO-1 via a similar mechanism (Nielsen *et al.*, 2002), and this is likely to be the case for α7Cx45 connexin as well (Kausalya *et al.*, 2001; Laing *et al.*, 2001). The human connexin family contains 20 members (Willecke *et al.*, 2002), and alignment study of the COOH-termini revealed that 9 members, none of which are from the β-class, contain potential ZO-1 binding motifs (Nielsen *et al.*, 2001). Because the molecular mechanism of ZO-1 binding appears similar in several connexins, there is a possibility that the biological function(s) of this interaction could also be similar for the different connexin isotypes.

Interactions of ZO-1 with Truncated Forms of α3Cx46 and α8Cx50 Connexins

Our results indicate that the truncated forms of α3Cx46 and α8Cx50 lacking the ZO-1 binding domains can still traffic and form structures between adjacent cells when expressed in nonpolarized HEK293 cells. This is in accordance with previous reports describing the expression of truncated forms of connexins.

A truncated form of α8Cx50 lacking the COOH-terminal domain forms gap junction channels with properties similar to wild-type channels, except for loss of pH_i sensitivity (Xu *et al.*, 2002). Truncated forms of α1Cx43 are also known to be able to form functional gap junctions when overexpressed in nonpolarized cells lines (Fishman *et al.*, 1991; Unger *et al.*, 1999). In contrast, α7Cx45 mutants lacking the ZO-1 binding site were reported not to localize to sites of cell–cell contact in polarized MDCK cells (Kausalya *et al.*, 2001). This discrepancy may be related to differences between polarized and nonpolarized cells. Another possibility is that the functional role of the ZO-1 interaction is dependent on the connexin isotype.

ZO-1 Involvement in Recycling of Connexins

For α1Cx43, mutants that no longer bind ZO-1 have been shown to exhibit an increased turnover rate (Toyofuku *et al.*, 2001). Furthermore, it has recently been shown that myocyte dissociation, which is known to promote gap junction remodeling, increased the association of ZO-1 with α1Cx43 (Barker *et al.*, 2002). These results suggest that the interaction of ZO-1 with α1Cx43 is involved in regulating the recycling of the connexin. A similar biological function has been ascribed to the interaction of the PDZ domain containing protein EBP50 (ezrinradixin–moesin–binding phosphoprotein-50) with β_2-adrenergic receptors. Disruption of this interaction inhibits β_2-adrenergic receptor recycling at the plasma membrane and leads to missorting of endocytosed β_2-adrenergic receptors to lysosomes (Hall *et al.*, 1998b). The lens is characterized by a slow but constant connexin turnover rate detected primarily at the equatorial cortical region, where the fiber junctions are assembled. ZO-1 may have a similar role in recycling of fiber gap junctions in this region of the lens.

The lens may serve as an excellent model system for studying these interactions because of its inherent properties. These include the possibilities of studying an intact, nonvital organ that expresses only a limited number of well-characterized connexins and the availability of knock-out mice lacking combinations of all connexins expressed in the lens.

ACKNOWLEDGMENTS

This work was supported by a grant from the Danish Research Council (to P.A.N.), National Institutes of Health grant EY-13605 (to N.M.K), National Eye Institute NEI Core Grant EY1792, and an Unrestricted Fund from Research to Prevent Blindness (RPB) to the University of Illinois at Chicago. The electron microscope study was supported by the ALCON award (to E.L.B.).

REFERENCES

Anderson, J.M., Stevenson, B.R., Jesaitis, L.A., Goodenough, D.A., and Mooseker, M.S. (1988). Characterization of ZO-1, a protein component of the tight junction from mouse liver and Madin-Darby canine kidney cells. J. Cell Biol. *106*, 1141–1149.

Barker, R.J., Price, R.L., and Gourdie, R.G. (2002). Increased association of ZO-1 with connexin43 during remodeling of cardiac gap junctions. Circ. Res. *90*, 317–324.

Baruch, A., Greenbaum, D., Levy, E.T., Nielsen, P.A., Gilula, N.B., Kumar, N.M., and Bogyo, M. (2001). Defining a link between gap

junction communication, proteolysis, and cataract formation. J. Biol. Chem. *276*, 28999–29006.

Baruch, Z.H., and Lim, W.A. (2001). Mechanism and role of PDZ domains in signaling complex assembly. J. Cell Sci. *114*, 3219–3231.

Bazzoni, G., Martinez-Estrada, O.M., Orsenigo, F., Cordenonsi, M., Citi, S., and Dejana, E. (2000). Interaction of junctional adhesion molecule with the tight junction components ZO-1, cingulin, and occludin. J. Biol. Chem. *275*, 20520–20526.

Benedetti, E.L., Dunia, I., Dufier, J.L., Yit, K.S., and Bloemendal, H. (1996). Plasma membrane-cytoskeleton complex in the normal and cataractous lens. In: Cytoskeleton, vol 3. London, UK: JAI Press, 451–518.

Benedetti, E.L., Dunia, I., Recouvreur, M., Nicolas, P., Kumar, N.M., and Bloemendal, H. (2000). Structural organization of gap junctions as revealed by freeze-fracture and SDS fracture-labeling. Eur. J. Cell Biol. *79*, 575–82.

Dev, K.K., Nakanishi, S., and Henley, J.M. (2001). Regulation of mglu(7) receptors by proteins that interact with the intracellular C-terminus. Trends Pharmacol. Sci. *22*, 355–361.

Dunia, I., Recouvreur, M., Nicolas, P., Kumar, N., Bloemendal, H., and Benedetti, E.L. (1998). Assembly of connexins and MP26 in lens fiber plasma membranes studied by SDS-fracture immunolabeling. J. Cell Sci. *111*, 109–120.

Dunia, I., Recouvreur, M., Nicolas, P., Kumar, N.M., Bloemendal, H., and Benedetti, E.L. (2001). Sodium dodecyl sulfate-freeze-fracture immunolabeling of gap junctions. Methods Mol. Biol. *154*, 33–55.

Fanning, A.S., and Anderson, J.M. (1999). Protein modules as organizers of membrane structure. Curr. Opin. Cell Biol. *11*, 432–439.

Fanning, A.S., Jameson, B.J., Jesaitis, L.A., and Anderson, J.M. (1998). The tight junction protein ZO-1 establishes a link between the transmembrane protein occludin and the actin cytoskeleton. J. Biol. Chem. *273*, 29745–29753.

Fishman, G.I., Moreno, A.P., Spray, D.C., and Leinwand, L.A. (1991). Functional analysis of human cardiac gap junction channel mutants. Proc. Natl. Acad. Sci. USA *88*, 3525–3529.

Giepmans, B.N., and Moolenaar, W.H. (1998). The gap junction protein connexin43 interacts with the second PDZ domain of the zona occludens-1 protein. Curr. Biol. *8*, 931–934.

Giepmans, B.N., Verlaan, I., and Moolenaar, W.H. (2001). Connexin-43 interactions with ZO-1 and alpha- and beta-tubulin. Cell Adhes. Commun. *8*, 219–223.

Gong, X., Li, E., Klier, G., Huang, Q., Wu, Y., Lei, H., Kumar, N.M., Horwitz, J., and Gilula, N.B. (1997). Disruption of alpha3 connexin gene leads to proteolysis and cataractogenesis in mice. Cell *91*, 833–843.

Gonzalez-Mariscal, L., *et al*. (1999). Molecular characterization of the tight junction protein ZO-1 in MDCK cells. Exp. Cell. Res. *248*, 97–109.

Gruijters, W.T., Kistler, J., and Bullivant, S. (1987). Formation, distribution and dissociation of intercellular junctions in the lens. J. Cell Sci. *88*(Pt 3), 351–359.

Guerrier, A., Fonlupt, P., Morand, I., Rabilloud, R., Audebet, C., Krutovskikh, V., Gros, D., Rousset, B., and Munari-Silem, Y. (1995). Gap junctions and cell polarity: connexin32 and connexin43 expressed in polarized thyroid epithelial cells assemble into separate gap junctions, which are located in distinct regions of the lateral plasma membrane domain. J. Cell Sci. *108*, 2609–2617.

Hall, R.A., Ostedgaard, L.S., Premont, R.T., Blitzer, J.T., Rahman, N., Welsh, M.J., and Lefkowitz, R.J. (1998a). A C-terminal motif found in the beta2-adrenergic receptor, P2Y1 receptor and cystic fibrosis transmembrane conductance regulator determines binding to the Na^+/H^+ exchanger regulatory factor family of PDZ proteins. Proc. Natl. Acad. Sci. USA *95*, 8496–8501.

Hall, R.A., *et al*. (1998b). The beta2-adrenergic receptor interacts with the Na^+/H^+-exchanger regulatory factor to control Na^+/H^+ exchange. Nature *392*, 626–630.

Itoh, M., Nagafuchi, A., Moroi, S., and Tsukita, S. (1997). Involvement of ZO-1 in cadherin-based cell adhesion through its direct binding to alpha catenin and actin filaments. J. Cell Biol. *138*, 181–192.

Itoh, M., Nagafuchi, A., Yonemura, S., Kitani-Yasuda, T., Tsukita, S., and Tsukita, S. (1993). The 220-kD protein colocalizing with cadherins in non-epithelial cells is identical to ZO-1, a tight junction-associated protein in epithelial cells: cDNA cloning and immunoelectron microscopy. J. Cell Biol. *121*, 491–502.

Jiang, J.X., and Goodenough, D.A. (1996). Heteromeric connexons in lens gap junction channels. Proc. Natl. Acad. Sci. USA *93*, 1287–1291.

Kausalya, P.J., Reichert, M., and Hunziker, W. (2001). Connexin45 directly binds to ZO-1 and localizes to the tight junction region in epithelial MDCK cells. FEBS Lett. *505*, 92–96.

Kim, E., Niethammer, M., Rothschild, A., Jan, Y.N., and Sheng, M. (1995). Clustering of Shaker-type K^+ channels by interaction with a family of membrane-associated guanylate kinases. Nature *378*, 85–88.

Kumar, N.M., and Gilula, N.B. (1996). The gap junction communication channel. Cell *84*, 381–388.

Laing, J.G., Manley-Markowski, R.N., Koval, M., Civitelli, R., and Steinberg, T.H. (2001). Connexin45 interacts with zonula occludens-1 and connexin43 in osteoblastic cells. J. Biol. Chem. *276*, 23051–23055.

Lo, W.K., Mills, A., and Kuck, J.F. (1994). Actin filament bundles are associated with fiber gap junctions in the primate lens. Exp. Eye Res. *58*, 189–96.

Mathias, R.T., Rae, J.L., and Baldo, G.J. (1997). Physiological properties of the normal lens. Physiol. Rev. *77*, 21–50.

Milks, L.C., Kumar, N.M., Houghten, R., Unwin, N., and Gilula, N.B. (1988). Topology of the 32-kd liver gap junction protein determined by site-directed antibody localizations. EMBO J. *7*, 2967–2975.

Moyer, B.D., *et al.* (2000). The PDZ-interacting domain of cystic fibrosis transmembrane conductance regulator is required for functional expression in the apical plasma membrane. J. Biol. Chem. *275*, 27069–27074.

Muth, T.R., Ahn, J., and Caplan, M.J. (1998). Identification of sorting determinants in the C-terminal cytoplasmic tails of the gamma-aminobutyric acid transporters GAT-2 and GAT-3. J. Biol. Chem. *273*, 25616–25627.

Nielsen, P.A., Baruch, A., Giepmans, B.N., and Kumar, N.M. (2001). Characterization of the association of connexins and ZO-1 in the lens. Cell Adhes. Commun. *8*, 213–217.

Nielsen, P.A., Beahm, D.L., Giepmans, B.N., Baruch, A., Hall, J.E., and Kumar, N.M. (2002). Molecular cloning, functional expression, and tissue distribution of a novel human gap junction forming protein, connexin-31.9. J. Biol. Chem. *277*, 38272–38283.

Paul, D.L., Ebihara, L., Takemoto, L.J., Swenson, K.I., and Goodenough, D.A. (1991). Connexin46, a novel lens gap junction protein, induces voltage-gated currents in nonjunctional plasma membrane of *Xenopus* oocytes. J. Cell Biol. *115*, 1077–1089.

Pari, G., Jardine, K., and McBurney, M.W. (1991). Multiple CArG boxes in the human cardiac actin gene promoter required for expression in embryonic cardiac muscle cells developing in vitro from embryonal carcinoma cells. Mol. Cell. Biol. *11*, 4796–4803.

Rajasekaran, A.K., Hojo, M., Huima, T., and Rodriguez-Boulan, E. (1996). Catenins and zonula occludens-1 form a complex during early stages in the assembly of tight junctions. J. Cell Biol. *132*, 451–463.

Sheng, M., and Sala, C. (2001). PDZ domains and the organization of supramolecular complexes. Annu. Rev. Neurosci. *24*, 1–29.

Songyang, Z., Fanning, A.S., Fu, C., Xu, J., Marfatia, S.M., Chishti, A.H., Crompton, A., Chan, A.C., Anderson, J.M., and Cantley, L.C. (1997). Recognition of unique carboxyl-terminal motifs by distinct PDZ domains. Science *275*, 73–77.

Stevenson, B.R., Siliciano, J.D., Mooseker, M.S., and Goodenough, D.A. (1986). Identification of ZO-1: a high molecular weight polypeptide associated with the tight junction (zonula occludens) in a variety of epithelia. J. Cell Biol. *103*, 755–766.

Tenbroek, E., Arneson, M., Jarvis, L., and Louis, C. (1992). The distribution of the fiber cell intrinsic membrane proteins MP20 and connexin46 in the bovine lens. J. Cell Sci. *103*, 245–257.

Toyofuku, T., Akamatsu, Y., Zhang, H., Kuzuya, T., Tada, M., and Hori, M. (2001). c-Src regulates the interaction between connexin-43 and ZO-1 in cardiac myocytes. J. Biol. Chem. *276*, 1780–1788.

Toyofuku, T., Yabuki, M., Otsu, K., Kuzuya, T., Hori, M., and Tada, M. (1998). Direct association of the gap junction protein connexin-43 with ZO-1 in cardiac myocytes. J. Biol. Chem. *273*, 12725–12731.

Unger, V.M., Kumar, N.M., Gilula, N.B., and Yeager, M. (1999). Expression, two-dimensional crystallization, and electron cryo-crystallography of recombinant gap junction membrane channels. J. Struct. Biol. *128*, 98–105.

White, T.W., Bruzzone, R., Goodenough, D.A., and Paul, D.L. (1992). Mouse Cx50, a functional member of the connexin family of gap junction proteins, is the lens fiber protein MP70. Mol. Biol. Cell *3*, 711–720.

White, T.W., Goodenough, D.A., and Paul, D.L. (1998). Targeted ablation of connexin50 in mice results in microphthalmia and zonular pulverulent cataracts. J. Cell Biol. *143*, 815–825.

Willecke, K., Eiberger, J., Degen, J., Eckardt, D., Romualdi, A., Güldenagel, M., Deutsch, U., and Söhl, G. (2002). Structural and functional diversity of connexin genes in the mouse and human genome. Biol. Chem. *383*, 725–737.

Xu, X., Berthoud, V.M., Beyer, E.C., and Ebihara, L. (2002). Functional role of the carboxyl terminal domain of human connexin 50 in gap junctional channels. J. Membr. Biol. *186*, 101–112.

Yeager, M., and Gilula, N.B. (1992). Membrane topology and quaternary structure of cardiac gap junction ion channels. J. Mol. Biol. *223*, 929–948.

Zampighi, G.A., Eskandari, S., and Kreman, M. (2000). Epithelial organization of the mammalian lens. Exp. Eye Res. *71*, 415–435.